D3.3: Augmented reality composite view creation and visualisation

SMARTsurg

Smart We**A**rable **R**obotic **T**eleoperated **surg**ery

3.3: Augmented Reality Composite View Creation and Visualisation

Due date: M18

Abstract: The present document is a deliverable of the SMARTsurg project, funded by the European Commission's Directorate-General for Research and Innovation (DG RTD), under its Horizon 2020 Research and innovation programme (H2020). This deliverable aims at presenting the results of Task T3.3 "*Augmented Reality Composite View Creation and Visualisation" until M18 of the project.* . This is a preliminary version of the deliverable's final version that will be provided by M28. Up to this state of Task 3.3, several state-of-the-art methods were examined, providing promising results for the surface co-registration procedure of the pre-operative data to the 3D reconstructed surgical area, whereas additional techniques will be examined and developed until the final version of this deliverable. Moreover, an automatic segmentation module was created in order to extract ground truth data for the evaluation of the aforementioned 3D registration approaches.

Dissemination Level		
PU	Public	x
PP	Restricted to other programme participants (including the Commission Services)	
RE	Restricted to a group specified by the consortium (including the Commission Services)	
CO	Confidential, only for members of the consortium (including the Commission Services)	

Document Status

Document Title	Augmented reality composite view creation and visualisation
Version	1.0
Work Package	3
Deliverable #	3.3
Prepared by	CERTH
Contributors	CERTH
Checked by	POLIMI
Approved by	UWE
Date	29/06/2018
Confidentiality	PU

Reference	:	SMARTsurg-WP3-D3.3-v0.3-CERTH
Version	:	0.3
Date	:	2018.06.22
Page	:	3

D3.3: Augmented reality composite view creation and visualisation

Contact Points

Coordinator		
	University of the West of England/ Bristol Robotics Laboratory T Building, Frenchay Campus BS16 1QY Bristol, UK	Tel: +44 117 32 81301 E-mail: Sanja.Dogramadzi@brl.ac.uk Website:www.brl.ac.uk/research/researchthemes/medicalrobotics.aspx

Partners		
	Centre for Research and Technology Hellas / Information Technologies Institute Building A - Office 1.1A 6th km Charilaou - Thermi, 57001 Thessaloniki, Greece	Tel.: +30 2311 257777 Fax: +30 2310 474128 E-mail: tzovaras@iti.gr Website:www.iti.gr
	Politecnico di Milano Department of Electronics, Information and Bioengineering Building 32.2 Via G.Ponzio 34/5 Milan, Italy	Tel.: +39 022 399 3371 E-mail: giancarlo.ferrigno@polimi.it Website:www.nearlab.polimi.it
	North Bristol National Health Service Trust/ Bristol Urological Institute Brunel Building, Southmead Hospital BS10 5NB Bristol, UK	Tel.: +44 117 4140898 E-mail: anthony.koupparis@nbt.nhs.uk Website: www.nbt.nhs.uk/bristol-urological-institute
	University of Bristol Translational Biomedical Research Centre Senate House, Tyndall Avenue BS8 1TH Bristol, UK	Tel.: +44 117 3423286 E-mail: r.ascione@bristol.ac.uk Website:www.bristol.ac.uk/health-sciences/research/tbrc
	European Institute of Oncology Division of Urology Via Ripamonti, 435 20141 Milan, Italy	Tel.: +39 0257489516 E-mail: ottavio.decobelli@ieo.it Website: www.ieo.it
	TheMIS Orthopaedic Center 6 Adrianoupoleos St. 55133 Thessaloniki, Greece	Tel.: +30 2310 223 113 E-mail: papacostas@the-mis.gr Website: www.the-mis.gr

D3.3: Augmented reality composite view creation and visualisation

	Cybernetix 306 Rue Albert Einstein 13882 Marseille, France	Tel.: +33 491 210 484 E-mail: jvandenbosch@cybernetix.fr Website: www.cybernetix.fr
	Optinvent R&D Department Avenue des Buttes de Coesmes 80 35700 Rennes, France	Tel.: +33 299871066 E-mail: khaled.sarayeddine@optinvent.com Website: www.optinvent.com
	HIT Hypertech Innovations 10PolytechneiouStr. 3083, Límassol, Cyprus	E-mail: contact@hit-innovations.com Website: www.hit-innovations.com

D3.3: Augmented reality composite view creation and visualisation

Document Change Log

Each change or set of changes made to this document will result in an increment to the version number of the document. This change log records the process and identifies for each version number of the document the modification(s), which caused the version number to be incremented.

Change Log	Version	Date
First draft	0.1	May 25, 2018
Updated	0.3	June 22, 2018
Updated with partner's feedback	0.7	June 28, 2018
Submitted	1.0	June 29, 2018

Table of Contents

D3.3: Augmented reality composite view creation and visualisation

List of Figures

D3.3: Augmented reality composite view creation and visualisation

List of Tables

Reference	:	SMARTsurg-WP3-D3.3-v0.3-CERTH
Version	:	0.3
Date	:	2018.06.22
Page	:	9

D3.3: Augmented reality composite view creation and visualisation

Executive Summary

The present document is a deliverable of the SMARTsurg project, funded by the European Commission's Directorate-General for Research and Innovation (DG RTD), under its Horizon 2020 Research and innovation programme (H2020). This deliverable aims at presenting the results of Task T3.3 "*Augmented reality composite view and visualization*". It is developed within the scope of WP3, responsible for determining "*Visual Feedback and Teleoperation for Robot-Assisted MIS*" *methods.*

As stated in the GA (1.1.3) the main objective of T3.3 is the extraction of virtual content and its co-registration to the 3D reconstructed surgical area. Task T3.3 uses as input the result of task T3.1 ("On-the-fly 3D reconstruction of the surgical field"), thus these tasks are closely related.

The current document describes the theoretical and practical research conducted up to this stage, regarding state-of-the-art registration of preoperative 3D models to real-time 3D camera feed.

At this stage of the SMARTsurg project (M18) we are presenting a preliminary version of the D3.3, which includes a detailed description of the registration of pre-operative 3D models constructed from CT and/or MRI data to 3D reconstructed surfaces provided by real-time binocular stereo methods that are currently under development and evaluation (T3.1) applied to intra-operative data. The suitability of the methods with respect to both their accuracy and their computational cost for use in the final system is yet to be determined. A more thorough presentation and description of registration of 3D models to real-time camera 3D view methods for the final system will be published in an updated version of deliverable D3.3 in M28.

Up to this stage, we have evaluated four state-of-the-art methods in order to achieve the registration of pre-operative to intra-operative data[1]. We firstly evaluated the simple ICP approach. The second point-set to point-set registration method was an implementation of Coherent Point Drift method, followed by two methods for surface to surface registration. Firstly optimal step non-rigid ICP was examined, followed by diffeomorphic non-rigid registration of shapes approach.

While our research is still ongoing, the initial evaluation showed a superiority of the point-set to point-set approaches to the methods that concerned surface to surface registration. This superiority was evident in rigid cases. As a future step we intent to research further data with elasticity and examine how the two methods that register surface data apply to non-rigid data.

---

[1] Part of this work has been submitted to IEEE IST 2018 conference for possible publication with the title "Intra-Operative 3D Registration of MIS Reconstructed Surfaces to Pre-Operative Models".

D3.3: Augmented reality composite view creation and visualisation

1 Introduction

1.1 Objective and Scope

The purpose of this deliverable (D3.3 – "*Augmented reality composite view and visualization*") is to present the theoretical and practical research conducted up to this stage (M18), is aiming at the creation of the AR composite views and their visualization to SMARTsurg smart glasses (assistant surgeon), and VR glasses (surgeon). Based on the user requirements defined in SMARTsurg Deliverable D2.1 [1], only composite views including the MIS surgical field are useful to the surgeons. Thus, our efforts in this tasks focus on the creation of composite views where the reconstructed 3D surfaces of the surgical field are matched to pre-operative 3D models of the corresponding anatomical structures. Therefore, the end goal of this research is to successfully register 3D models extracted from pre-operative data to real-time 3D endoscopic camera feed of the intra-operative field of view by utilizing and extending state-of-the-art surface registration algorithms.

Particularly this document outlines:

- Description of the framework for extracting the 3D models from pre-operative data.
- State-of-the-art methods for surface registration.
- State-of-the-art methods for surface registration within Augmented Reality (AR) systems for RAMIS procedures.
- Preliminary results of aforementioned methods on MIS datasets.
- Future work.

1.2 Document Structure

The document consists of the construction of a preliminary dataset with ground truth data for evaluation (Section 2), where we outline the workflow steps from extracting the 3D model, to segmentation procedure, and noise addition. In Section 3, we outline the state-of-the-art methods in 3D model registration of pre-operative to intra-operative data and present the four 3D registration methods we have evaluated for this period. These preliminary evaluation results for the aforementioned methods are presented in Section 4.

1.3 Reference Documents

[1] SMARTsurg D2.1, Deliverable "End-user requirements, use cases and application scenarios"

[2] W. Zeng and X. D. Gu, "Registration for 3D surfaces with large deformations using quasi-conformal curvature flow," CVPR 2011, Providence, RI, 2011, pp. 2457-2464.

[3] Simpfendörfer, Tobias &Baumhauer, Matthias & Müller, Michael & N Gutt, Carsten &Meinzer, Hans-Peter &Rassweiler, Jens &Guven, Selcuk&Teber, Dogu. (2011). Augmented Reality Visualization During Laparoscopic Radical Prostatectomy. Journal of endourology / Endourological Society

D3.3: Augmented reality composite view creation and visualisation

[4] Su, Li-Ming &Vagvolgyi, Balazs& Agarwal, Rahul &Reiley, Carol & Taylor, Russell & Hager, Gregory. (2009). Augmented Reality During Robot-assisted Laparoscopic Partial Nephrectomy: Toward Real-Time 3D-CT to Stereoscopic Video Registration. Urology.

[5] Pessaux, Patrick & Diana, Michele &Soler, Luc &Piardi, Tullio& Mutter, Didier &Marescaux, Jacques. (2014). Robotic duodenopancreatectomy assisted with augmented reality and real-time fluorescence guidance. Surgical endoscopy.

[6] Oktay, Ozan& Zhang, Li & Mansi, Tommaso&Mountney, Peter &Mewes, Philip &Nicolau, Stéphane&Soler, Luc. (2013). Biomechanically Driven Registration of Pre- to Intra-Operative 3D Images for Laparoscopic Surgery. Medical image computing and computer-assisted intervention : MICCAI . International Conference on Medical Image Computing and Computer-Assisted Intervention

[7] Figl, Michael &Rueckert, Daniel & Hawkes, David &Casula, Roberto & Hu, Mingxing& Pedro, Ose& Ping Zhang, Dong & Penney, Graeme & Bello, Fernando & Edwards, Philip. (2009). Image Guidance for Robotic Minimally Invasive Coronary Artery Bypass. Computerized medical imaging and graphic

[8] 3D Slicer, an open source software platform for medical image informatics, image processing, and three-dimensional visualization. [https://www.slicer.org/]

[9] "Least-Squares Fitting of Two 3-D Point Sets" Arun et. al. PAMI, 1987, 10.1109/TPAMI.1987.4767965.

[10] "Method for Registration of 3D Shapes", Besl and McKay, PAMI 1992.

[11] Amberg, B., Romdhani, S., & Vetter, T. (2007). Optimal Step Nonrigid ICP Algorithms for Surface Registration. 2007 IEEE Conference on Computer Vision and Pattern Recognition, 1-8.

[12] Myronenko, A., & Song, X. (2010). Point set registration: Coherent point drift. IEEE transactions on pattern analysis and machine intelligence, 32(12), 2262-2275.

[13] H. Guo, A. Rangarajan, S. Joshi and L. Younes, "Non-rigid registration of shapes via diffeomorphic point matching," 2004 2nd IEEE International Symposium on Biomedical Imaging: Nano to Macro (IEEE Cat No. 04EX821), 2004, pp. 924-927 Vol. 1. doi: 10.1109/ISBI.2004.1398690

[14] Zhang, X., Tan, X., Gao, X., Wu, D., Zhou, X., & Fujita, H. Non-rigid registration of multi-phase liver CT data using fully automated landmark detection and TPS deformation. Cluster Computing, 1-15.

[15] B. T. T. Yeo, M. R. Sabuncu, T. Vercauteren, N. Ayache, B. Fischl and P. Golland, "Spherical Demons: Fast Diffeomorphic Landmark-Free Surface Registration," in IEEE Transactions on Medical Imaging, vol. 29, no. 3, pp. 650-668, March 2010. doi: 10.1109/TMI.2009.2030797

[16] Ibanez L., Audette M., Yeo B.T., Golland P. Rotational Registration of Spherical Surfaces Represented as QuadEdge Meshes. 2010 Apr.

D3.3: Augmented reality composite view creation and visualisation

[17]   Luo, B., & Hancock, E. R. (2002). Iterative procrustes alignment with the em algorithm. *Image and Vision Computing*, *20*(5-6), 377-396

1.4 Acronyms and Abbreviations

Abbreviation	Definition
AR	Augmented Reality
D	Deliverable
GA	Grant Agreement
EC	European Commission
DMP	Data Management Plan
M	Month
MIS	Minimally Invasive Surgery
WP	Work package
SoA	State of the art
DoA	Description of Action
MRI	Magnetic Resonance Imaging
CT	Computed Tomography
RAMIS	Robot-Assisted Minimally Invasive Surgery
ICP	Iterative Closest Point
CPD	Coherent Point Drift
TRUS	Transrectal Ultrasonography
GMM	Gaussian Mixture Model
FLER	Fluorescence-Based Enhanced Reality
FEM	Finite Element Method
RMS	Root Mean Squared

D3.3: Augmented reality composite view creation and visualisation

2 Extraction of 3D models from Pre-operative Data

Taking into account all the information provided by the patients' pre-operative examinations is crucial for a positive outcome of an MIS procedure. Medical imaging (CT, MRI) are used to extract information of the surgical field prior to the surgery. In order to make valuable use of this information within an augmented reality module we can extract 3D models of the anatomical areas of interest.

2.1 3D model extraction using 3D Slicer

The 3DSlicer software [8], was used to review pre-operative CT images of a knee phantom in order to extract the 3D model of the anatomical structure of meniscus. We had different meniscus models scanned within the knee phantom corresponding to various meniscus lacerations as also a sample corresponding to a healthy meniscus. All CT images were reviewed and the anatomical structure of interest was manually annotated within the 3D Slicer software for each CT image series. The corresponding annotations were used to create a 3D representation of the marked area as a surface model for every meniscus model. These models are treated as the pre-operative "ground-truth" data, and are used in the Augmented Reality module of SMARTsurg framework.

The 3D Slicer environment and the manual annotations, together with the corresponding 3D model for the "healthy" model and for one "torn meniscus" model can be seen in Figure 1 and Figure 2 bellow accordingly.
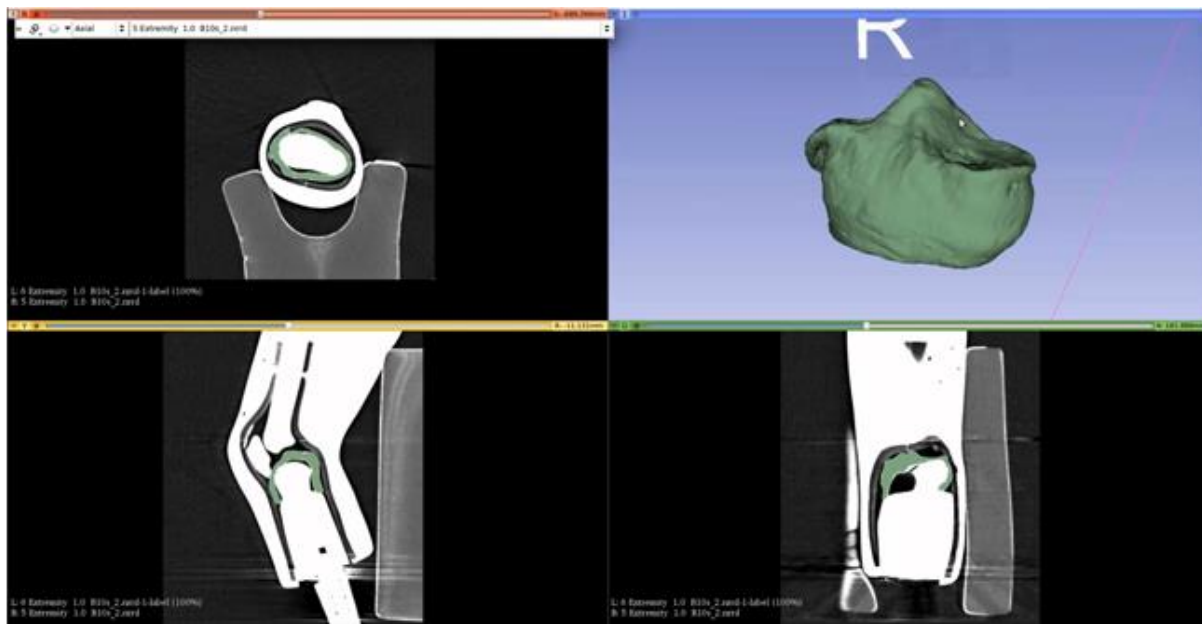
Figure 1. 3D Slicer software environment showing the annotation of a healthy sample. An expert reviews the CT scans and manually annotates the phantom meniscus model in any of the CT planes

D3.3: Augmented reality composite view creation and visualisation

(axial, coronal, sagittal). The corresponding area is then automatically annotated in the other two views and also in the 3D model.
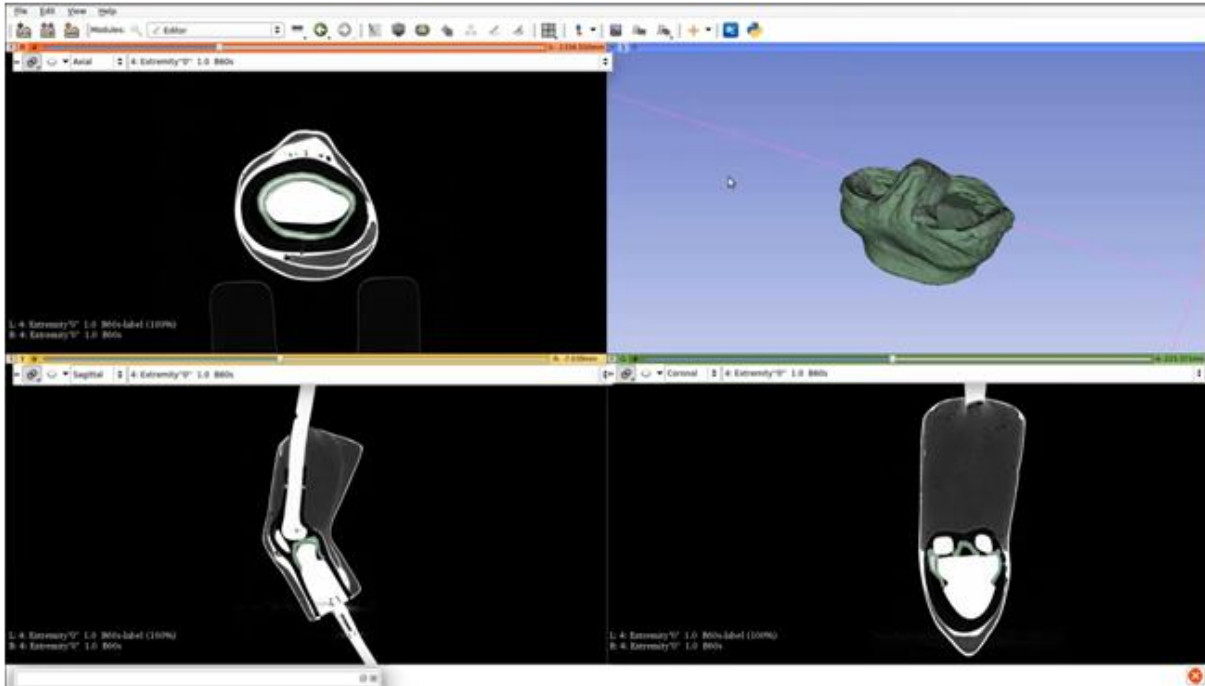
Figure 2. 3D Slicer software environment showing the annotation of a torn meniscus sample.

Through the manual annotation, as described previously, a 3D mesh model is extracted that describes in great detail the pre-operative anatomical region of interest and is used by the Augmented Reality module. The 3D models of the aforementioned two examples (healthy, torn) of phantom meniscus can be seen in greater detail in Figure 3.

Figure 3
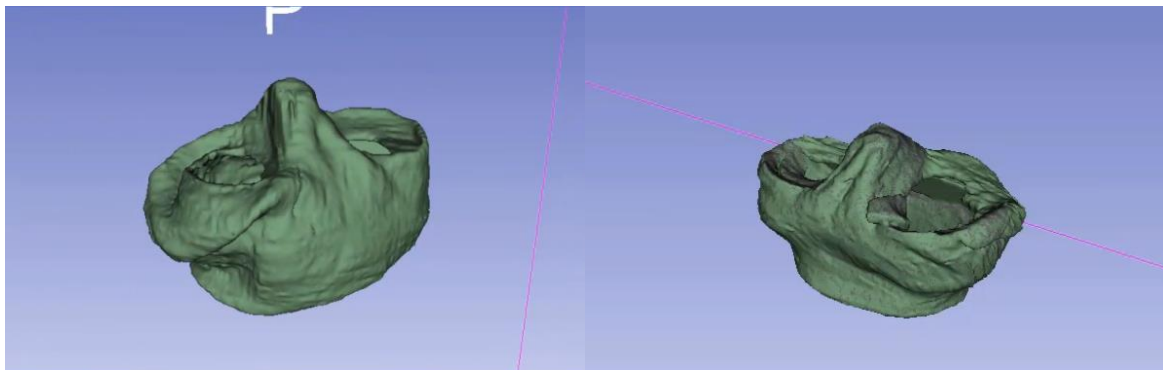
Figure 3. Healthy (left) and torn (right) meniscus 3D models, extracted through manual annotation in 3D Slicer software.

D3.3: Augmented reality composite view creation and visualisation

2.2 Extraction of ground truth samples from pre-operative 3D models

Using the pre-operative 3D models acquired through the procedure described in the previous section, we developed a framework for segmenting these models to smaller sections for testing the examined surface registration algorithms.

Since the anatomical structure of interest during the MIS procedure will most probably be occluded during the registration the need of registering small parts of the pre-operative model to the field of view was created. The framework we created can segment the 3D model in smaller areas, extracting small parts of the surface and keeping information regarding the initial model and the area where the segment was extracted. Using this knowledge, we can extract information regarding the success of the registration by measuring the distance of the initial vertices of the "ground truth" model and the corresponding ones in the surface part that is being registered.

In order to create a preliminary dataset, we used the mesh model of a healthy meniscus, extracted though manual annotation of the meniscus anatomy on every slice inside 3D Slicer software. Using 25 unique random points on the model as seeds for the segmentation, 50 segmented regions were extracted that had from 15% to 50% of overlapping between them. For every seed we used two different values (1.5cm and 2.5cm) as radius, to determine the size of the segmented patch. Every patch was stored both in point-set and surface form. As an extra feature, noise was added to the models in order to simulate noisy input data from the On-the-fly 3D reconstruction of the surgical field. As an initial step for noise simulation we used used a trivariate Gaussian distribution ($\mu = 0.0$, $\sigma = 0.06$). Where 1σ distance (0.6mm) in each dimension, corresponds roughly to a total of about 1mm error distance. The average Root Mean Square (RMS) error between the points of the produced noisy models and the points of initial ones is 1.56 mm. The procedure described above has been automated and performed within the ROS framework.

A sample of the segmentation result including added noise can be seen in Figure 4. For each segmented area a mesh file is created as well as a corresponding file containing the IDs of the vertices from the initial model that are included in the segment.
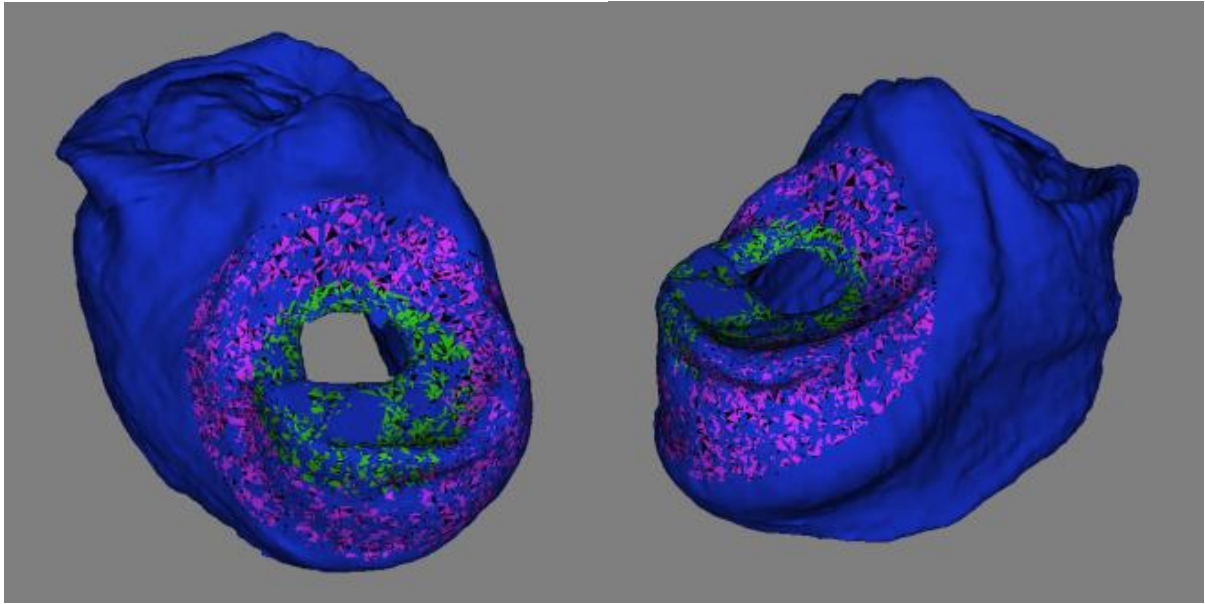
Figure 4. Automatic segmentation of 3D model for ground truth extraction. The 3D pre-operative model (blue) is segmented in smaller regions (magenta, green) to simulate occlusions at the in-operative view.

	Reference	:	SMARTsurg-WP3-D3.3-v0.3-CERTH
	Version	:	0.3
	Date	:	2018.06.22
	Page	:	17

D3.3: Augmented reality composite view creation and visualisation

3 Surface Registration Methods for Augmented Reality MIS

3.1 State of the Art

There are many existing research works trying to apply AR in MIS to help overcome some of the current limitations. The general call is for on-the-fly fusion between other modalities of the MIS system and the MIS video, creating a composite view that conveys additional information (such as the location of important subsurface structures).

Previous works can be broadly divided into two categories, those that tackle the problem with semi-automatic approach and those that use a more constraint and automatic one. In works where a semi-automatic approach is adopted, either the surgeon roughly aligns the 3D model to the camera view as an initialization step, or on-tissue artificial markers are being utilized for assisting the registration process.

Simpfendörferet al. in their paper *"Augmented Reality Visualization During Laparoscopic Radical Prostatectomy"* [3] propose a marker assisted 2D-3D point correspondence registration of Transrectal Ultrasonography (TRUS) data to real time video feed. Custom-developed needles with colored heads that are placed into the prostate surface as soon as the organ is exposed play the role of markers. These navigation aids are segmented in three-dimensional (3D) TRUS data that is acquired right after their placement and then are continuously by the surgical navigation system. The markers are tracked in real time and the registration between TRUS image and laparoscopic video is computed through two dimensional to three dimensional (2D-3D) point correspondences.

Figl et al. in *"Image guidance for robotic minimally invasive coronary artery bypass"* [7]constructed a 4D motion model of the heart and achieved registration in two phases; first the temporal alignment is achieved and then the spatial alignment follows. Spatial alignment is done manually by the surgeon at the beginning of the procedure, and the correspondence points are computed based on photo-consistency. Having established temporal registration from the first phase, the remaining motion is considered to be rigid apart from possible deformation of the heart due to breathing function. The main parameters for the 4D motion model, heart rate and respiratory frequency were determined through image processing. By comparing one of the images of the beating heart within a video sequence with all the others they were able to determine the parameters using cross-correlation as a similarity measure. The frequencies were then found as peaks in the Fourier transform of this function.

Li-Ming et al. in *"Augmented Reality During Robot-assisted Laparoscopic Partial Nephrectomy: Toward Real-Time 3D-CT to Stereoscopic Video Registration" [4]*present a modified ICP registration method based on selected on model 3D reference positions. In the initialization step an operator selected the surface points to be traced. Since the 3D surface reconstructed from the stereo video provided only a partial view of the kidney; the ICP variant approach used firstly estimated the visibility of the preoperative 3D model in the current view

		Reference	:	SMARTsurg-WP3-D3.3-v0.3-CERTH
		Version	:	0.3
		Date	:	2018.06.22
		Page	:	18

D3.3: Augmented reality composite view creation and visualisation

before each iteration to restrict the point correspondence search only to the visible area of the organ.

Apart from the semi-automatic methods already described, there have been many works that adopted an automatic approach.W. Zeng and X. D. Gu in their article "*Registration for 3D surfaces with large deformations using quasi-conformal curvature flow" [2]*presented the first method of large deformation surface 3D registration by solving Beltrami equations based on describing deformations with quasiconformal mappings. Their proposed approach is general, global optimal, and robust. It can search for the desired registration in the complete space of diffeomorphisms, such as rigid motions, isometric transformations or conformal mappings. The global optimum is determined by the method unique up to a 3 dimensional transformation group, it can handle large surfaces with complicated topologies.

Pessaux et al. in *"Robotic duodenopancreatectomy assisted with augmented reality and real-time fluorescence guidance" [5]*suggested the use of fluorescence videography instead of model to real-time video feed registration. They proposed the fluorescence-based enhanced reality (FLER) in which they present the fusion of fluorescence videography with AR to guide the intestinal resection and assess the vascular supply at the future anastomotic site.

Oktayet al. in *"Biomechanically Driven Registration of Pre- to Intra-Operative 3D Images for Laparoscopic Surgery" [6]*propose the computation and use of an insufflation model for their diffeomorphic non-rigid registration, which is a dense matching method driven by the gradient of local cross correlation similarity measure. As a first step the deformations and organ shifts caused by gas pressure as computed, using a biomechanical model, which is based on the mechanical parameters and pressure level. This model is used to achieve an initial alignment with intra-operative images. This initial registration step accounts for both non-rigid and rigid transformations caused by the insufflation. The applied model couples the parameters with an intensity similarity measure and the finite element method (FEM) registration methods. At the next step the diffeomorphic registration takes places, which having a higher degree of freedom refines the surface differences between the pre-operative image, warped according to the biomechanical model, and the intra-operative image.

We have researched and applied several automatic surface registration methods, as described in the next sections, from simple rigid registration to more complex techniques where the deformations of the tissue is taken into account.

3.2 Point and surface based registration, and Iterative Closest Point

As a first attempt traditional ICP algorithms for rigid registration where tested. Two approaches where researched. A point based one [9], where the 3D model and the 3D reconstructed image from the stereoscopic laparoscopic camera are treated as point clouds with no surface information. Thus the registration is treated as a minimization problem, where the Root Mean Squared (RMS) distance between corresponding points once aligned has to be minimized.

	Reference	:	SMARTsurg-WP3-D3.3-v0.3-CERTH
	Version	:	0.3
	Date	:	2018.06.22
	Page	:	19

D3.3: Augmented reality composite view creation and visualisation

The second attempt is a variant of ICP [10]where a set of initial rotation and translation states is used to avoid the main problem of the ICP algorithm, convergence in local minima.

While the ICP may produce very good registration results with registration error < 1mm, the time need for registration is increased dramatically when the number of points increases, thus making it prohibitive for on-the-fly registration. An additional disadvantage of such techniques is that they do not take into account the deformations of the organ surface due to organ movement or by its interaction with the surgical instruments. Finally the basic ICP algorithm does not produce optimal registration results when the target 3D scene is occluded (by other tissues or surgical instruments).

3.3 Optimal Step Non-rigid ICP Algorithm for Surface Registration

Trying to overcome the aforementioned constraints of the traditional ICP method, an extension of the ICP framework to non-rigid registration was also tested [11]. While retaining the convergence properties of the original ICP algorithm the optimal step non-rigid ICP framework allows the use of different regularizations. The algorithm takes into account various stiffness weights and respectively deforms the template surface towards the target one. With this approach, the whole range of global and local deformations is recovered. For each stiffness weight, the optimal iterative closest point steps are being used to achieve the optimal corresponding deformation. For every step at first a nearest-point search is being applied in order to estimate the preliminary correspondences. Then the optimal deformation of the template is calculated taking into account the fixed correspondences computed at the first step as well as the active stiffness weight. This procedure continues iteratively with new correspondences found by searching from the displaced template vertices. Locally affine regularization is being applied, by assigning an affine transformation to each vertex and minimizing the difference in the transformation for the neighboring vertices. It is shown that by using this regularization method the optimal deformation for the fixed correspondences and a fixed stiffness can be accurately determined with efficiency. The method achieves very good registration results for a wide range of initial conditions, and handles missing data robustly. More details regarding this approach can be found in [11].

3.4 Coherent Point Drift point set registration

A related problem to surface-based registration is point set registration. These two different approaches are used interchangeably in the literature. Rigorously speaking, surface-based registration deals with surfaces that have connectivity information. On the other hand point set based registration deals with sets of points without any connectivity information. The Coherent Point Drift (CPD) algorithm [12], is a probabilistic method utilized for both rigid and non-rigid point set registration. The registration problem is being formulated as a probability density estimation problem, where one point set is represented using a Gaussian Mixture Model (GMM) and the other point set is observations from aforementioned GMM. The GMM centroids (representing the first point set) are being fitted to the data (the second point set) by maximizing the likelihood. The GMM centroids are being forced to move as a group

D3.3: Augmented reality composite view creation and visualisation

coherently in order the topological structure of the point sets to be preserved. In the rigid case, a closed form solution derived from the maximization step of the EM algorithm [17] is used for optimization of the likelihood function, where the parameters of the GMM centroid locations are being re-configured so the coherence constrained can be imposed. In the other hand, in the non-rigid case the coherence constraint is imposed by regularizing the displacement field and using variational calculus to derive the optimal transformation. The CPD algorithm can perform with great accuracy for both rigid and non-rigid transformations and can cope with the presence of noise, outliers and missing points. Through this evaluation process only the non-rigid case was examined More details regarding this approach can be found in [12].

3.5 Diffeomorphic non-rigid registration of shapes

Diffeomorphisms are broadly used in non-rigid methods for registration where large deformations are expected. Usually the methodology refers to point-set registration methods, but in [13] authors have shown that diffeomorphisms can be used to registered 3D shapes also by utilizing a point-set representation for shapes since statistical shape analysis in this space is relatively straight forward. A joint clustering and diffeomorphism estimation strategy was introduced, allowing the simultaneous estimation of the correspondence and the fitting of a diffeomorphism between two point-sets.

Basically, within the proposed strategy the centers of the corresponding clusters for each point-set are always in consistency since they are sharing same index. In the course of clustering, the cluster center counterparts in each point-set are linked by a diffeomorphism and as a consequence are forced to move in lock-step with one another. More information regarding this method can be found in [13].
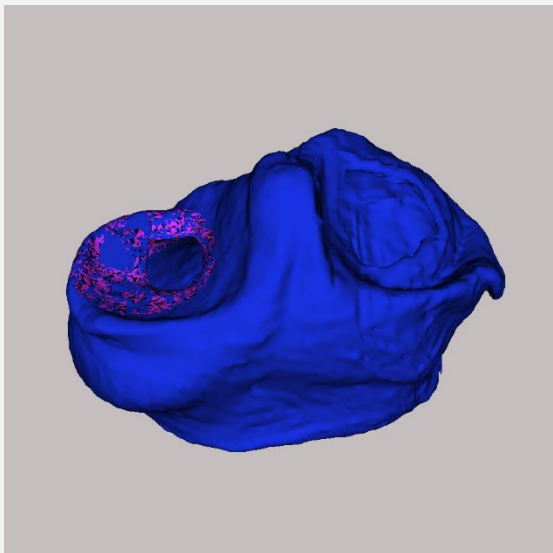
		Reference	:	SMARTsurg-WP3-D3.3-v0.3-CERTH
		Version	:	0.3
		Date	:	2018.06.22
		Page	:	21

D3.3: Augmented reality composite view creation and visualisation

4 Methods' Evaluation

4.1 Ground truth dataset of meniscus phantom

In order to evaluate the described methods in the previous section, the segmentation framework we developed (section 2.2 in this document) was utilized to extract testing surfaces with ground truth data. A dataset that included segmentations of various sizes and added noise was created. For every segment in this dataset, both mesh and point-set models were extracted so the all aforementioned methods (for point-set and surface registration methods) could be evaluated on the same baseline data. Samples of this dataset can be seen in Figure 5 bellow.

Segmented Region (mesh)	**Segmented Region (point-set)**

		Reference	:	SMARTsurg-WP3-D3.3-v0.3-CERTH
		Version	:	0.3
		Date	:	2018.06.22
		Page	:	22
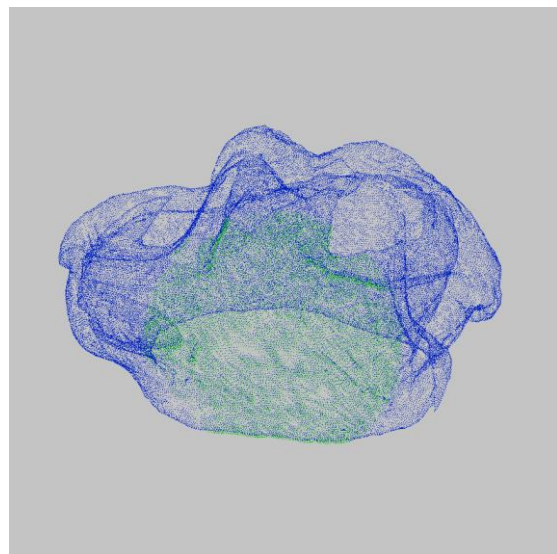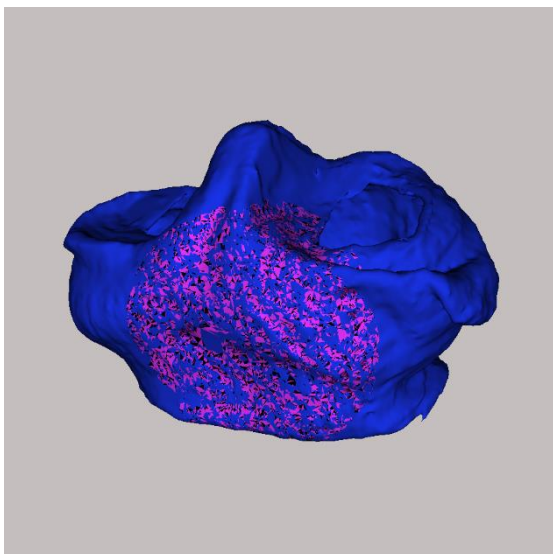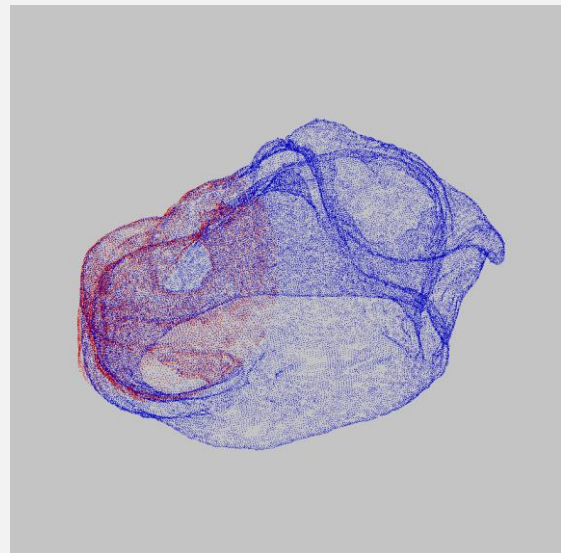
D3.3: Augmented reality composite view creation and visualisation
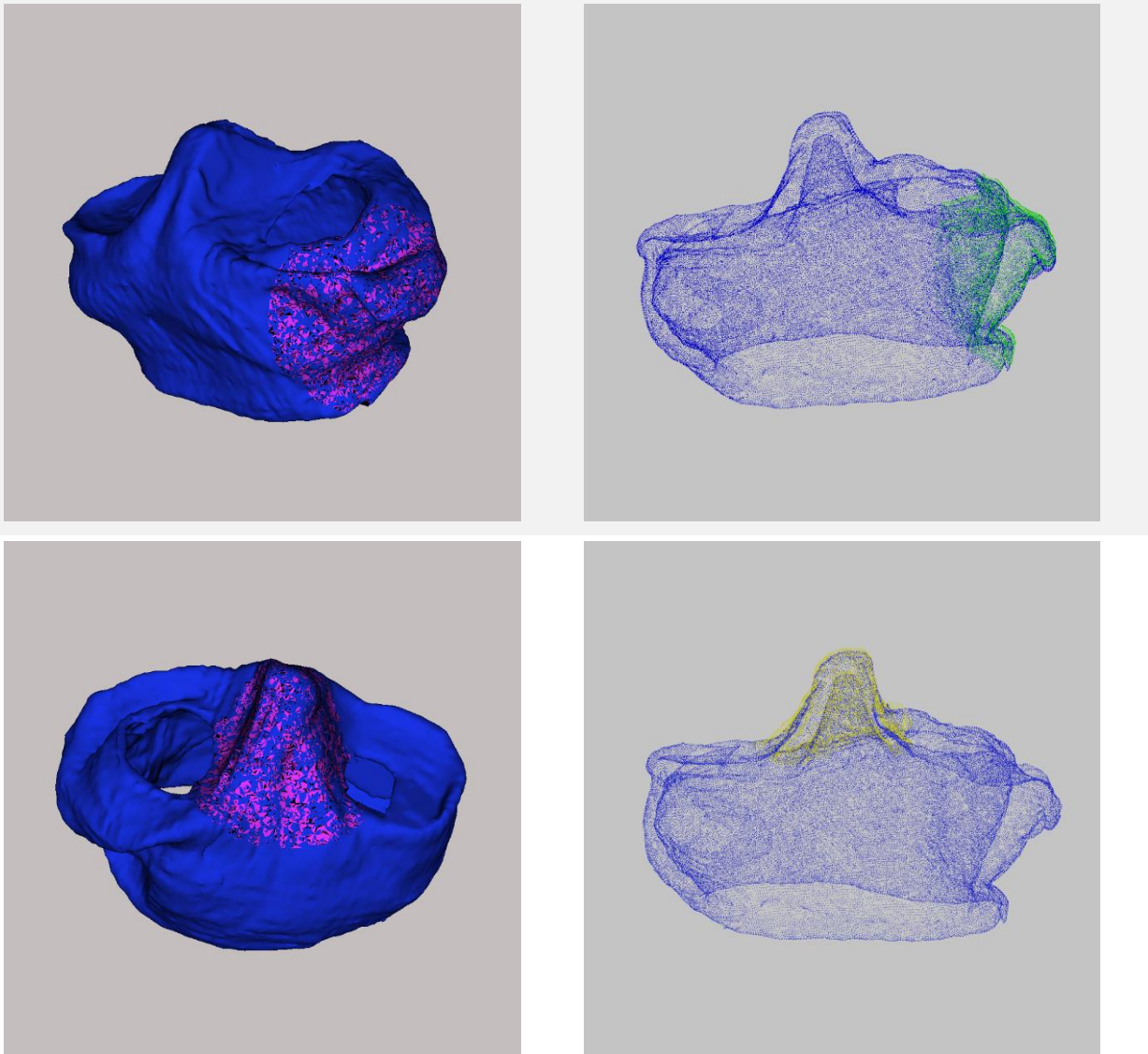
Figure 5. Examples of segmentations from the constructed ground truth dataset, resulting from a 3D model of a healthy meniscus phantom. For every segmented region a mesh (first column) and a point-set representation (second column) is extracted. The initial model and the sample segmentation are represented with different colours.

4.2 Preliminary Evaluation Results

Using the aforementioned dataset all methods described in section 3 were evaluated at the same base. Both point-based and surface-based methods achieved good registration accuracy in several cases, and failed at other ones. We used RMS as a metric to define the correctness of a registration. Since we have ground truth information for all patches in our dataset, we can measure the root mean squared distance of all points/vertices in the template patch to the corresponding ones of the target surface/point-set. We determined a

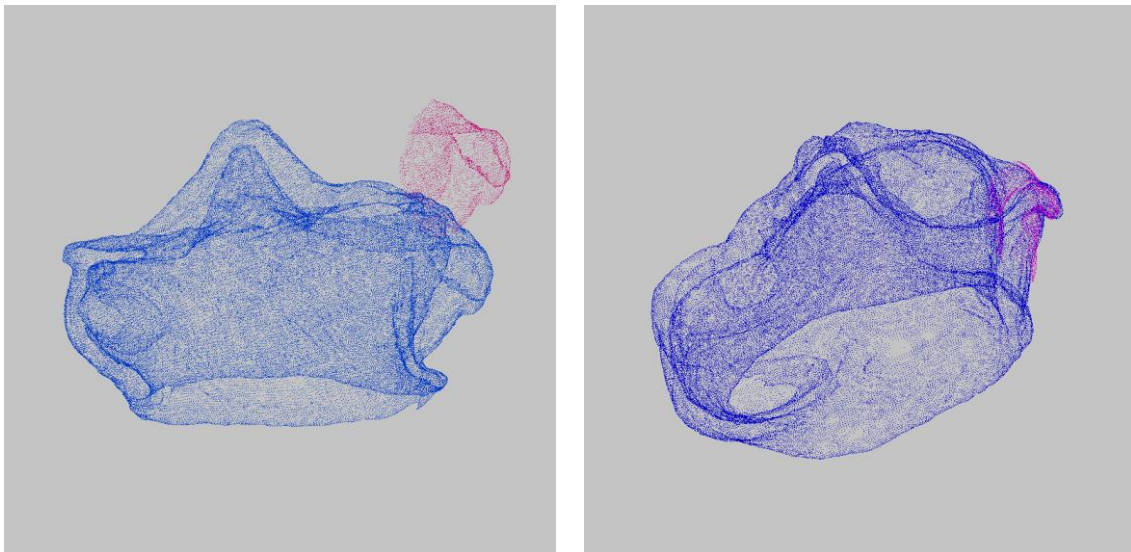**D3.3: Augmented reality composite view creation and visualisation**

value of RMS < 2 mm to be our threshold for considering a registration as successful. Besides the noise level, and the actual size of the segmented region, the initial position of the template point-set/surface with respect to the target was also parameterized to simulate various initialization errors. The segmented patch was translated and rotated at random distance and orientation in all three axis in every iteration, A detailed evaluation for each approach follows.

4.2.1 ICP approach

This basic approach managed to achieve acceptable registration results to most of the cases with an average convergence error (RMS distance) of 1.92mm. Through all the examined patches of the dataset, ICP achieved a successful registration in 67.3% of the cases. Although the registration was successful in the majority of the cases, the time needed for converging was one of the highest amongst all, since the average converging time was 2.28 sec. The cases where this approach didn't achieve acceptable results were due to large initial distance between the two point-sets, thus leading to local minima after a few initial iterations. Despite that, ICP managed to achieve an acceptable registration even when the template patch had a distance of 2.4 cm from the target. Examples of good and bad registration results using the ICP approach can be seen in Figure 6.

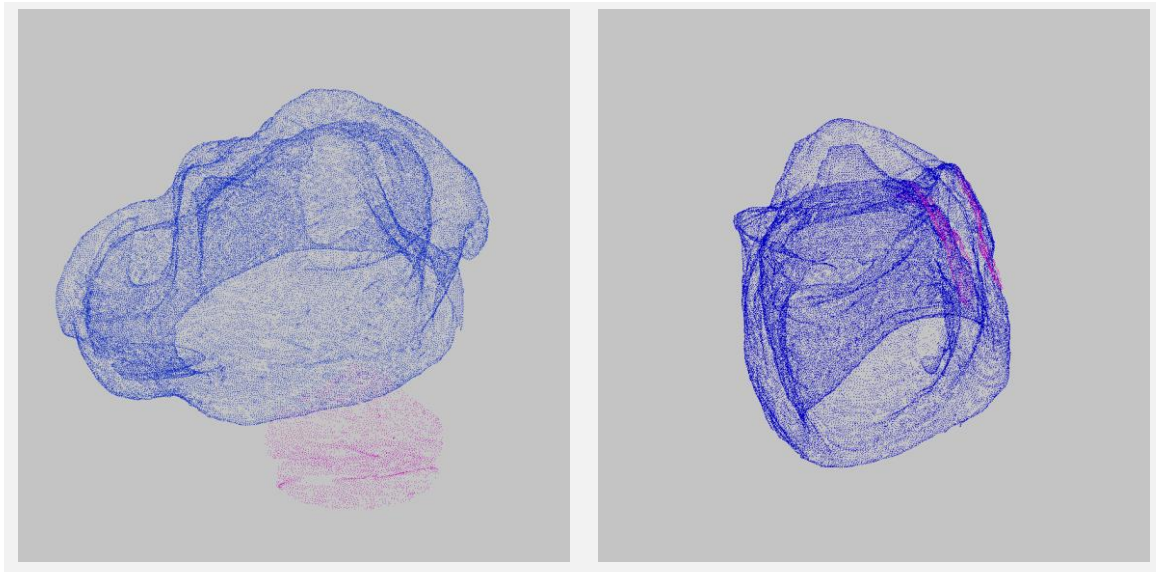**D3.3: Augmented reality composite view creation and visualisation**

Figure 6. Examples of good and bad registration results using ICP algorithm for registering the two point-sets. The initial position of the template with respect to the target point-set is shown in the first column. A successful registration result with convergence score $< 10^{-3}$ is shown on the right of the first row, while an erroneous registration result with convergence score > 2 is shown on the right of the second row.

4.2.2 Optimal Step Non-Rigid ICP

This ICP variant for surfaces achieved similar results with the simple ICP algorithm achieving an overall success rate of 72.6%. The time needed for registration was again too high reaching an average of 2.53 sec to complete the registration. The average convergence error was 1.84mm. The registration was successful in the majority of the cases, even in those including high rate of noise. The cases where this approach didn't achieve acceptable results were again due to large initial distance between the two point-sets, but this method was more sensitive to the initial distance between the template patch and the target one, since the maximum distance between the two patches, that this method achieved a successful registration (RMS < 2mm) was 1.3 cm. Examples of successful and erroneous registration results using the optimal step non-rigid ICP approach can be seen in Figure 7.

Figure 7

	Reference	:	SMARTsurg-WP3-D3.3-v0.3-CERTH
	Version	:	0.3
	Date	:	2018.06.22
	Page	:	25

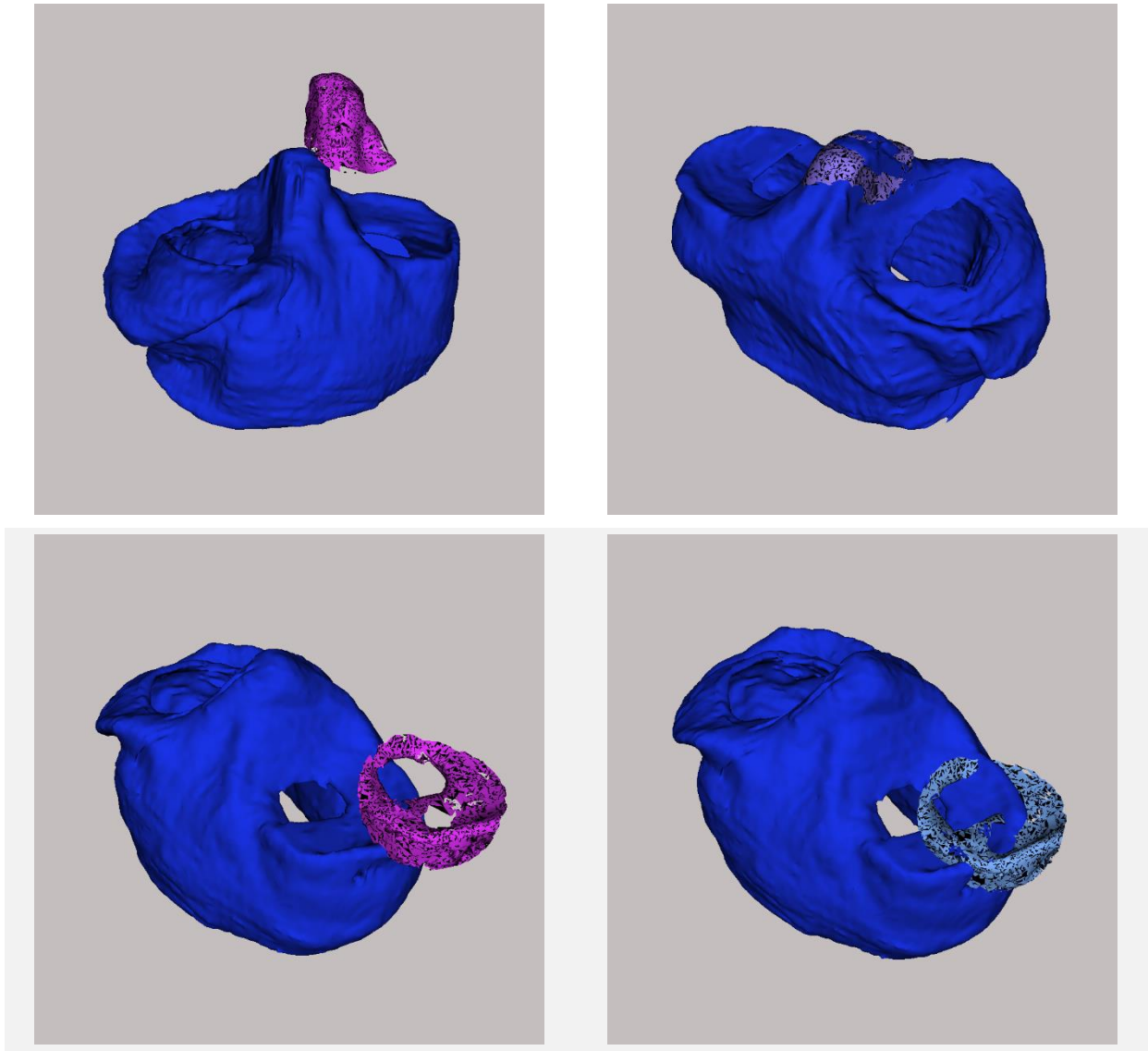**D3.3: Augmented reality composite view creation and visualisation**

Figure 7. Examples of good and bad registration results using optimal non-rigid ICP algorithm for registering the two surfaces. The initial position of the template with respect to the target surface is shown in the first column. A successful registration result with convergence error $< 10^{-3}$ is shown on the right of the first row, while an erroneous registration result with convergence error > 2.3 mm is shown on the right of the second row.

4.2.3 Coherent Point Drift

This approach managed to achieve the best registration results with an average convergence error of 1.76 mm and an overall success rate of 78.8%. It outperformed all other three candidates and is considered a strong candidate for the SMARTsurg 3D registration framework. Although the registration wasn't successful in all of the cases, it managed to achieve the lowest registration error amongst all examined methods. The cases where this approach didn't achieve a good result were actually again due to large initial

D3.3: Augmented reality composite view creation and visualisation

distance between the two point-sets, by achieving acceptable registration with a maximum average distance of 1.8 cm between the two point sets. The average time for registration was 1.57 sec, which is not yet acceptable for a real time framework but the method can be further parametrized trying to reach real-time registration times. Examples of good and bad registration results using the CPD approach can be seen in Figure 8.

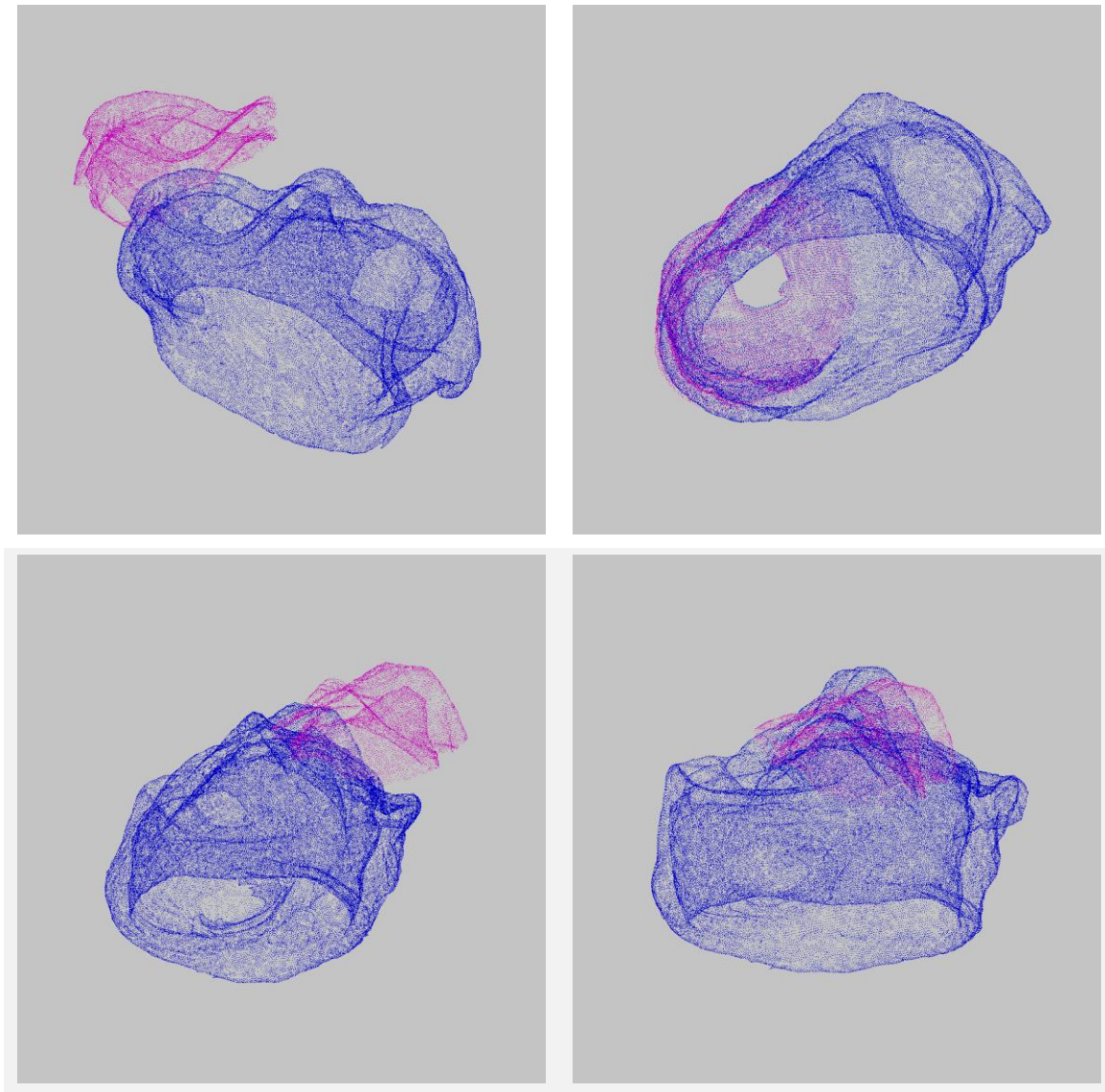Figure 8. Examples of successful and erroneous registration results using CPD algorithm for registering the two point-sets. The initial position of the template with respect to the target point-set is shown in the first column. A good registration result with convergence error < 10^{-4} is shown on the right of the first row, while a bad registration results with convergence error > 2.4 is shown on the right of the second row.

D3.3: Augmented reality composite view creation and visualisation

4.2.4 Diffeomorphic non-rigid registration of shapes

This approach achieved the lowest acceptable registration success rate of 49.8%, with an average convergence error of 2.63mm. The time needed for registration was even higher than the ICP reaching an average of 2.74 sec for converging.. The average time needed for convergence was near ICP time, reaching 2.74 sec. The initial distance between the two surfaces didn't seem to cause any drawback in the registration process since the maximum distance for which this method achieved an acceptable registration reached up to 4.1 cm. Examples of successful and erroneous registration results using the Diffeomorphic non-rigid registration of shapes approach can be seen in Figure 9.
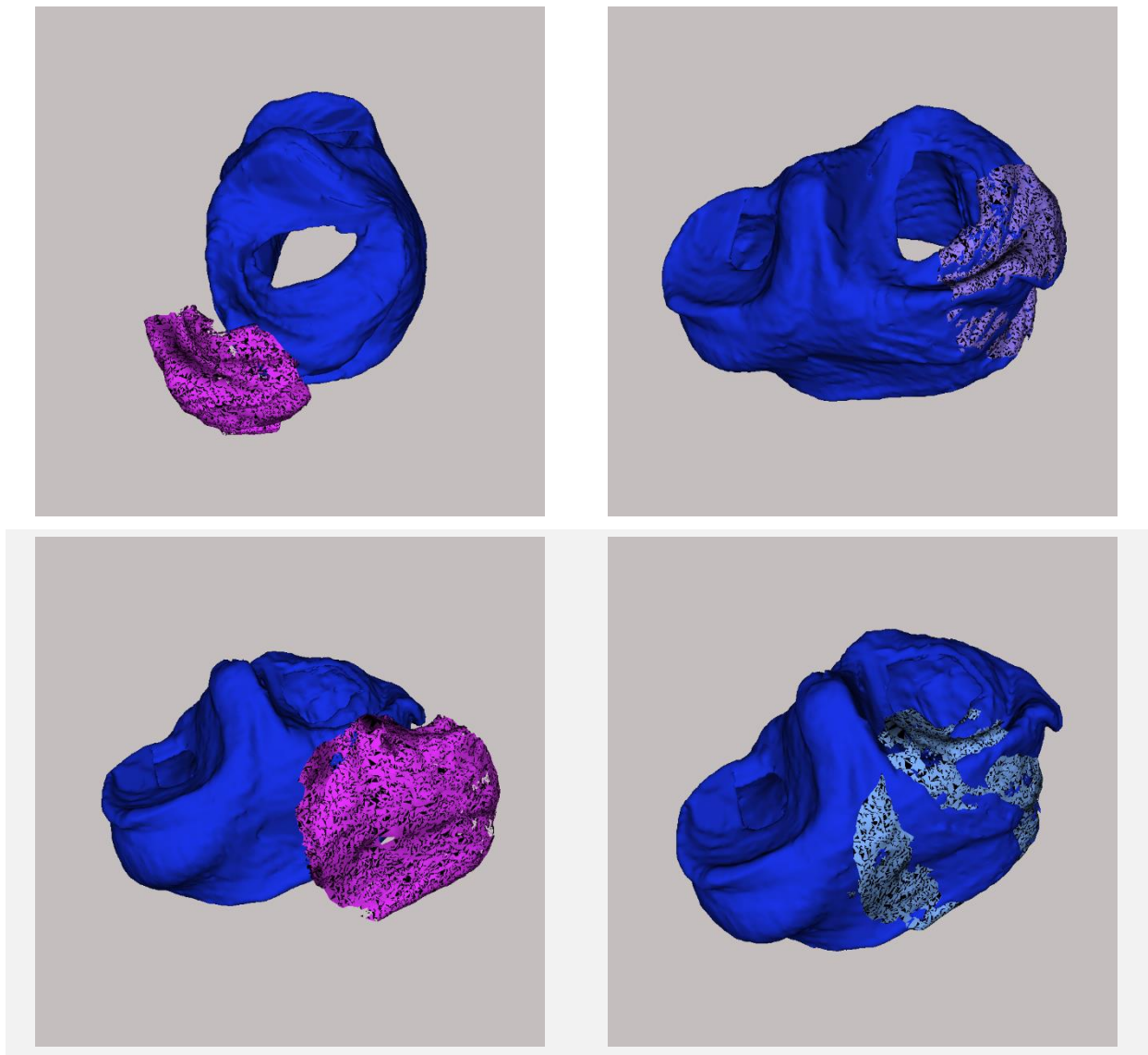

Figure 9. Examples of good and bad registration results using Diffeomorphic non-rigid registration of shapes algorithm for registering the two surfaces. The initial position of the template with respect to the target surface is shown in the first column. A successful registration result with convergence error

D3.3: Augmented reality composite view creation and visualisation

< 10⁻² mm is shown on the right of the first row, while an erroneous registration result with convergence error > 2.7mm is shown on the right of the second row.

4.2.5 Overall evaluation results

Through this evaluation process we extracted some crucial information for our next steps. By examining the parameters that make each method to end in an erroneous registration result it is clear that a good initialization step is critical. In the majority of the cases where the registration was achieved with a large registration error the initial position of the template with respect to the target was larger than the ones that the registration was successful.

The results these methods showed are promising, but we are going to research further in the parameterization to achieve better results. Another critical point we should investigate further is the optimization of the registration process with respect of execution time, since the final objective of this framework is to collaborate in real time with the On-the-fly 3D reconstruction of the surgical field framework.

Moreover, during this preliminary research only small deformations of the template surface/point-set were examined. It is crucial to examine larger deformation since the organ surface during the surgical process will undergo large deformations due to interaction with the surgical instruments. An overall evaluation report of the examined methods can be seen in Table 1. As indicated by these results the CPD approach not only outperforms the other tested methods with respect to success rate and average RMS error, but is also the fastest.

	Success Rate %	Average convergence error (RMS)	Maximum initial distance	Average Registration Time
ICP	67.3%	1.92mm	2.4 cm	2.28 sec
Optimal Step Non-Rigid ICP	72.6%	1.84mm	1.3 cm	2.53 sec
CPD (non-rigid case)	**78.8%**	**1.76mm**	1.8 cm	**1.57 sec**
Diffeomorphic	49.8%	2.63mm	**4.1 cm**	2.74 sec

Table 1. Overall evaluation results for the examined methods. CPD achieved the lowest average registration error of 1.76 mm as well as the best average registration time (1.57 sec), and success rate since it achieved an acceptable registration in 78.8% of the cases. Diffeomorphic non-rigid registration of shape ICP and CPD achieved the two lowest registration errors, as well as the two highest success rates, but had high average time needed for the registration. Diffeomorphic non-rigid registration of shapes scored the highest average registration error, but can be highly parameterized and will be examined more to this end.

D3.3: Augmented reality composite view creation and visualisation

5 Future Work

This document describes the preliminary results of the research we conducted in state-of-the-art methods for 3D surface registration. We will continue researching methods in this field up until M28 of the project, when an updated version of deliverable D3.3 will be provided.

We are currently in an effort to create a larger dataset, which will include models from different types of meniscus, but also different types of organs so we will be able to evaluate the examined methods in a more complete aspect. In this extended dataset we intend to add different types and amounts of noise.

During this preliminary research, we only evaluated the examined methods in rigid transformations, and there is a possibility that this is the reason the point-set to point-set methods outperformed the surface to surface ones. In the future, we aim to add non-rigid samples in the ground truth dataset, containing a scale of small to large deformations, we believe that in those cases the surface to surface registration methods will be more dominant.

In general, apart from modifying accordingly the investigated methods for performing within the real-time framework of SMARTsurg, we will continue our efforts on the development of our own proposal for a novel surface registration method. Moreover, additional state-of-the-art methods will also be examined, such as Spherical Demons: Fast Diffeomorphic Landmark-Free Surface Registration [15], and Rotational registration of spherical surfaces represented as quadedge meshes [16].

In [15] the fast Spherical Demons algorithm for registering spherical images are presented. This work showed that the two-step optimization of the Demons algorithm can also be applied on the sphere. By utilizing the one parameter subgroups of diffeomorphisms, the resulting deformation is invertible. The algorithm was extensively tested in two different applications showing very promising results. In [16] they have proposed a solution to register two meshes of spherical topology and geometry. In practice, this is the second part of a processing pipeline whose first part would be a spherical mapping of a mesh of arbitrary geometry but of spherical geometry (genus 0). The proposed solution is a rigid registration based on the scalars attached to the mesh.

Both approaches can be used for performing registration between two spherical meshes, although these contributions are not restricted to be used on spherical meshes, thus proving to be good candidates for future research in the context of SMARTsurg project.

After the investigation of all suitable techniques we intent to determine the most appropriate method for the projects' constraints and limitations, by selecting the approach that best suits for on-the-fly registration in real time camera view and produces the best registration results taking into account noisy data.

Finally, the resulting implementation will be optimized and a ROS interface will be created in order for the registration framework to be fully integrated with the On-the-fly 3D reconstruction of the surgical field framework produced within T3.1.

D3.3: Augmented reality composite view creation and visualisation

6 Conclusion

This report presented the SMARTsurg theoretical and practical research conducted up to this stage (M18), regarding state-of-the-art surface registration algorithms in terms of *Augmented reality composite view and visualization* framework*.*

As a first step for evaluation a ground truth dataset, containing both point-sets and meshes, was created from a healthy meniscus phantom. In the future this dataset is to be augmented with data from more meniscus phantoms with different states of damage, as also from more organ phantoms. We evaluated both point-set to point-set and surface-to-surface registration methods in the aforementioned ground truth dataset.

As a result of applying the evaluated methodologies to our ground truth dataset, we have identified the main problems we are going to encounter in the system and broke them down into steps for future examination. Mainly non-rigid cases should be examined using larger amounts of noise in the future. And the most important note we have extracted from this preliminary research is the need to find a method that could work in real time since the "*Augmented reality composite view and visualization*" component has to be working in collaboration with the "*On-the-fly 3D reconstruction of the surgical field*" component of T3.1.